Neuroscience 141 (2006) 1585–1597

NEURAL CORRELATES OF PRIMING ON OCCLUDED FIGURE INTERPRETATION IN HUMAN FUSIFORM CORTEX

L. C. LIU,[a]* G. PLOMP,[b] C. VAN LEEUWEN[b] AND A. A. IOANNIDES[a]

[a]*Laboratory for Human Brain Dynamics, RIKEN Brain Science Institute (BSI), 2-1 Hirosawa, Wakoshi, Saitama 351-0198, Japan*

[b]*Laboratory for Perceptual Dynamics, RIKEN Brain Science Institute, 2-1 Hirosawa, Wakoshi, Saitama 351-0198, Japan*

Abstract—The visual system rapidly completes a partially occluded figure. We probed the completion process by using priming in combination with neuroimaging techniques. Priming leads to more efficient visual processing and thus a reduction in neural activity in relevant brain areas. These areas were studied with high spatial resolution and temporal accuracy with focus on early perceptual processing. We recorded magnetoencephalographic responses from 10 human volunteers in a primed same–different task for test figures. The test figures were preceded by a sequence of two figures, a prime or control figure followed by an occluded figure. The prime figures were one of three possible interpretations of the occluded figures: global and local completions and mosaic interpretation. A significant priming effect was evident: in primed trials as compared with control trials, subjects responded faster and the latency was shorter in the magnetoencephalographic signal for the largest peak between 50 and 300 ms after the occluded figure onset. Tomographic and statistical parametric mapping analyses revealed stages of activation in occipitotemporal areas during occluded figure processing. Notably, we found significantly reduced activation in the right fusiform cortex between 120 and 200 ms after occluded figure onset for primed trials as compared with control trials. We also found significant spatiotemporal differences of local, global and mosaic interpretations for individual subjects but not across subjects. We conclude that modulation of activity in the right fusiform cortex may be a neural correlate of priming in the interpretation of an occluded figure, and that this area acts as a hub for different occluded figure interpretations in this early stage of perception.

Key words: priming, occlusion, magnetoencephalography, fusiform gyrus, perception, magnetic field tomography.

Our visual system rapidly completes a figure that is partially hidden behind its occluder. We are usually not aware that this involves selecting one out of, in principle, infinitely many possible completions. Different views exist on how the visual system is able to do this, depending on which properties of the occluded parts are considered relevant. Some explanations emphasize local properties of the occluded figure near the occluded region, such as good continuation (Kanizsa and Gerbino, 1982; Kellman and Shipley, 1991), others emphasize global properties of the occluded figure, such as symmetry (Buffart and Leeuwenberg, 1981), and still others assume that both local and global features play a role in completion (van Lier et al., 1995). In addition, an occluded figure together with its occluder could be seen as a mosaic without any occlusion. Hereafter we will use the term occluded figure interpretations to refer to the wider class of representations that encompasses local and global completions as well as mosaic representations of an occluded figure.

Behavioral studies have shown that responses to occluded figures can effectively be primed by their previously viewed unoccluded counterparts (Joseph and Nakayama, 1999; Zemel et al., 2002). Priming leads to faster or more accurate processing of stimulus information, following prior experience with the same or a related stimulus (Tulving and Schacter, 1990). In neuroimaging studies, this is reflected in a decrease in neural response to previously seen stimuli, compared with novel ones. Most likely, this is because less neural activity is required to process a stimulus after earlier exposure (Henson, 2003). In the present study, we used priming as a tool to study how the visual system settles on an occluded figure interpretation. We recognize from the outset that occluded figure interpretation may involve brain activity in multiple neuronal networks operating in parallel across time (Murray et al., 2004). Nevertheless, key nodes may exist that at specific times act as hubs in the network when figure interpretation is resolved. If this is the case, priming an occluded figure interpretation should show up as a reduction in activity in one or more specific areas. In the simplest case, when one node at one time is involved for all three interpretations, we would be able to determine when and where the visual system develops a bias for one of the three possible interpretations. Alternatively, each interpretation may have its own specialized area and time, a prospect consistent with the demonstration that the mosaic interpretation can precede completion (Sekuler and Palmer, 1992).

To address the question of where and when occluded figures are interpreted in the brain, we used a priming paradigm in combination with neuroimaging. In most priming studies, the primed figure is also the decision target of the task. Therefore in principle, priming may also influence some brain areas at a later stage of the process, for instance during a decision making stage. Some of the areas

*Corresponding author. Tel: +81-48-467-7218; fax: +81-48-467-9731.
E-mail address: lichan@brain.riken.jp (L. C. Liu).

Abbreviations: ERP, event-related potential; FG, fusiform gyrus; FS, filled square; G, global figure; IC, illusory contour; ICA, independent component analysis; ISI, inter-stimulus interval; L, local figure; LOC, lateral occipital complex; M, mosaic figure; MEG, magnetoencephalography; MFT, magnetic field tomography; ROI, region of interest; RT, reaction time; SNR, signal-to-noise ratio; SQ, square control figure.

0306-4522/06$30.00+0.00 © 2006 IBRO. Published by Elsevier Ltd. All rights reserved.
doi:10.1016/j.neuroscience.2006.04.062

involved in these later stages of processing may be the same as the ones involved in occluded figure interpretation. As a result, one cannot determine whether the primed response reflects perceptual facilitation of occluded figure interpretation or a later cognitive state. In order to separate priming from decision processes as much as possible, we used a procedure introduced by Stins and van Leeuwen (1993). Instead of having a single prime preceding a target, a sequence of two primes preceded the target in each trial. Both the first and second primes can facilitate the response to the target. If they do so independently, the facilitation effects on the target will add up. Alternatively, the first prime may influence processing of the second and hence together produce a super-additive effect on the target. In this case, the first stimulus must have facilitated the second, prior to the onset of target-related processes. This technique, therefore, enables us to observe priming relations among non-target stimuli.

In the present study, we focused our analysis of brain activity on the second stimulus and studied how it was primed by different first stimuli. We chose a procedure in which a simple figure was presented as a prime before a composite figure. The composite figure contained an occluded shape that can be interpreted, in principle, in at least three different ways: through local or global completion, or as a mosaic figure. The preceding simple figure was related to one of these three interpretations, so that it could bias the interpretation of the occluded figure. This bias was restricted to the following three conditions: (1) the simple figure should be presented before the composite figure, (2) the simple figure should be a possible interpretation of the composite figure and (3) the second composite figure should be presented briefly for 50 ms (Plomp and van Leeuwen, in press).

Although the experimental design in the present study is optimized to investigate early priming effects, stimuli are not precluded from further processing. We therefore need a neuroimaging technique with high spatial and temporal resolution to observe these early processes uncontaminated by later cognitive processing or accumulated effects of different processes. We used magnetoencephalography (MEG) to investigate neural correlates of priming on occluded figure interpretation by comparing the MEG responses to primed and non-primed composite figures. We used statistical parametric mapping in conjunction with magnetic field tomography (MFT) to characterize responses at all points in peristimulus time throughout the brain. We found significantly reduced activity in the right fusiform cortex between 120 and 200 ms after composite figure onset in primed as compared with control trials. Thus we localized the effect of priming on the perceptual interpretation of occluded figures in the right fusiform cortex. This applied to all alternative figure interpretations under investigation, global and local completions as well as mosaic interpretation. In a separate analysis of the MEG signal we identified a stronger peak with a slightly earlier latency for the evoked response of the second composite figure when it was preceded by mosaic as compared with either local or global first figures (Plomp et al., in press). In the present study, we compared the tomographic estimates of brain activity for the three different occluded figure interpretations and found significant spatiotemporal differences for individual subjects but no common area and latency for all subjects together. We conclude that modulation of activity in the right fusiform cortex is a neural correlate of priming in the interpretation of an occluded figure, and that this area acts as a hub for different occluded figure interpretations in early stage of perception.

EXPERIMENTAL PROCEDURES

Subjects

Ten healthy right-handed male subjects (mean age 35, range 25–62) volunteered for the MEG experiment. All subjects had normal or corrected-to-normal visual acuity and provided written informed consent to the experimental procedures as approved by the RIKEN Research Ethical Committee.

Experimental design

The experiment had three types of runs: task, figure baseline and task baseline runs. In a *task run*, each trial comprised three visual stimuli: a prime and two targets. Subjects were shown the three stimuli in rapid succession. The first stimulus (the prime) was either a simple figure (Fig. 1A) or a control figure (Fig. 1B). The second stimulus (the first target) was a composite figure consisting of a square partially occluding either a cross or a circle (Fig. 1A). This figure was ambiguous and could be interpreted in three ways, corresponding to the three simple figures. The interpretation could therefore be “primed” by the simple figure used as the first stimulus. The simple figures were: global (G), local (L) or mosaic (M) (Fig. 1A). Both global and local primes were based on amodal completion; occluded parts of a complete figure appear present even though the perceiver has no visual sensation of them. The global prime maximizes the number of symmetry axes of the occluded figure while the local prime keeps continuous lines at the points of occlusion. The mosaic prime resembled a puzzle-cut figure (i.e. no amodal completion). Hereafter the composite figures are referred to as figure A (“occluded cross”) or B (“occluded circle”), and their corresponding preceding simple figures as AG, AL, AM, BG, BL and BM. The percentages of figure area occlusion were as follows: AG 25%, AL 15%, BG 22% and BL 32%. The control figures were: a square (SQ) or two small, separated filled squares (FS) (Fig. 1B). SQ was the same as the square contained in the subsequent composite figure and hence primed some of the features of the composite. If priming of the occluded figure interpretation was effectively priming of figure features, then this control condition would have reproduced similar effects to a simple figure. The small squares of FS were located at the virtual centers of the two figures, mimicking their general locations and directions in the composite figure. The squares thus primed for the occurrence of a composite figure, providing a cue that a composite was about to appear at this particular position. They serve as control for attentional effects on the evoked response. The third stimulus (the second target) comprised a pair of simple figures and cued a same–different judgment about their relative figure shape. Fig. 1C shows the temporal sequence of a task trial. Both the first and second stimuli were presented for 50 ms with an inter-stimulus interval (ISI) of 300 ms. The presentation time of 50 ms is above the critical duration for which presentation time no longer influences visual acuity (Bartlett, 1965). Five hundred milliseconds after the second stimulus offset, the test figure was shown for one second. Before the first stimulus onset and during the ISI, a fixation dot was presented for 300–500 ms. After the offset of the test figure, subjects were given visual feedback on the screen

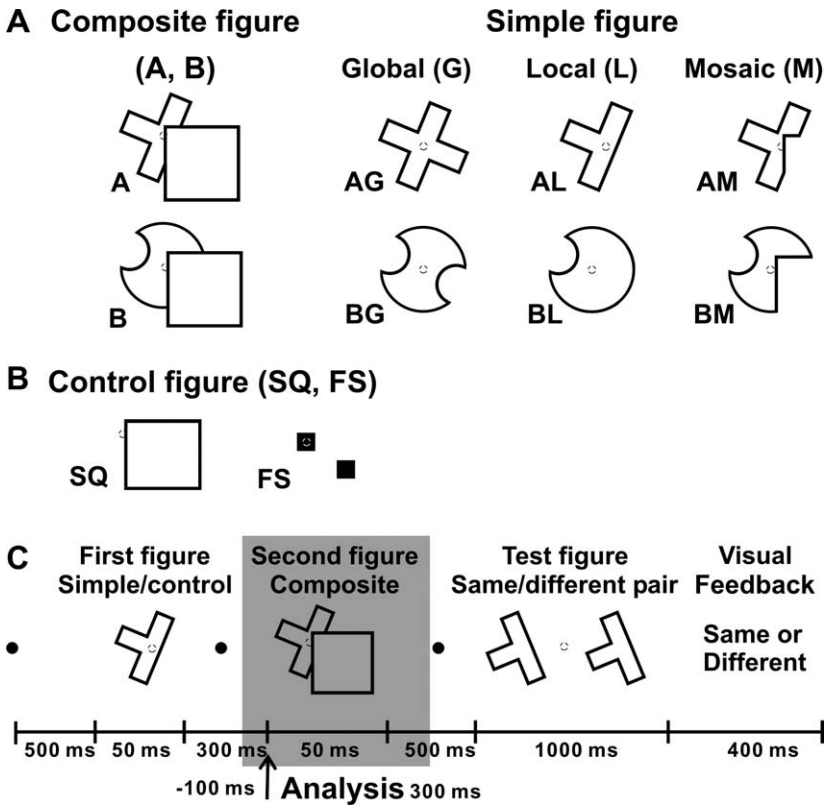

Fig. 1. Experimental design. (A) Examples of composite and simple figures. Simple figures are three interpretations (global, local and mosaic) of the occluded cross or circle in the composite figures. (B) Two control figures: SQ and FS. (C) The temporal sequence of a task run. The shaded area highlights the time period for the MEG data analysis, 100 ms before to 300 ms after the composite figure onset. For reference, the dotted circle in each panel indicates the fixation at the central location of the screen; this was not visible to subjects during the experiment.

followed by a blank (gray) screen presented for 200 ms to mark the end of a trial. Then the next trial began.

In the present MEG study, we analyzed the MEG response to the first target (the second stimulus, as highlighted by the gray box in Fig. 1C) and used the second target (the third stimulus) to establish priming behaviorally.

Sixteen task runs were recorded for each subject. There were 64 trials in each run, 8 trials for each of the simple and control figures (AG, AL, AM, BG, BL, BM, SQ and FS). The composite figure was either figure A or B, congruent with the preceding first stimulus. If the first stimulus was SQ or FS, the composite was either A or B, counterbalanced across all 16 runs. Within a run, half of the test figures consisted of "same" pairs, the other half of "different" pairs. The test figure was constructed from the six simple figures (AG, AL, AM, BG, BL and BM) but was rotated counterclockwise from the original ones to minimize the effect of overlapping features on subject responses.

In a *task baseline run*, the temporal sequence was the same as in task runs, except both the first and second stimuli were replaced with a blank screen (shown for 50 ms). Subjects fixated on the center of the screen and responded to test figures by lifting the left or right index finger. There were 48 trials in each run and six runs were recorded. One baseline run was recorded after every two task runs. We compared subject behavior responses to the test figure from task baseline runs with those from task runs to establish the first and second stimuli primed responses to the third stimulus when the first two figures were related to the third.

The order of task and task baseline runs, and the assignment of left-right index finger for same–different judgment were counterbalanced across all 10 subjects. In both the task runs and task baseline runs, since a test figure was shown for 1 s followed by a visual feedback, reaction times (RT) longer than 1.2 s were rejected in the behavioral data analysis. We also rejected trials with RT less than 250 ms or with multiple responses. The rejection rate was 0.2%.

In a *figure baseline run*, subjects were instructed to view attentively the first simple or control figure (AG, AL, AM, BG, BL, BM, SQ, FS) followed by a blank screen (instead of a composite figure as in the task runs). After the blank screen, the fixation dot appeared for 500 ms, and then the next trial started. There were 64 trials in each run, 8 trials each for the above eight first stimulus types. Two figure baseline runs were recorded for each subject, once before and once after the 16 task runs and the 6 task baseline runs. We analyzed the MEG response to the blank screen from the figure baseline runs.

All stimuli were shown in black outlines on a gray background (contrast 87%) and were presented pseudo-randomly within each run. The stimuli subtended the following visual angles: simple and composite figures, 2.5×2.5°; left and right figures in the test figure, 2.5×2.5° with center-to-center distance of 4.5° along the horizontal meridian; fixation dot, 0.2°.

Equipment setup

The subjects sat on a comfortable chair inside a magnetically shielded room and were instructed to fixate on the center of a screen (about 56 cm away) throughout the course of each run (about 4 min). The stimuli were presented using an XGA LCD projector (refresh rate of 60 Hz) and back-projected onto the screen center using a mirror system. A photodiode was attached to the screen to mark the exact onset time of each stimulus.

MEG signal recording

We recorded MEG signals using a whole-head Omega 151-channel system (CTF Systems Inc., Vancouver, BC, Canada) with additional electrodes to monitor artifacts from vertical and horizontal eye movements and heart function. The eye movements were monitored using one pair of EOG electrodes 1 cm above and below the left eye (vertical movement) and another pair 1 cm lateral to the left and right outer canthus of the eyes (horizontal movement). The heart function was monitored using ECG electrodes, placed at left and right wrists, left and right ankles and lead V2. The MEG signal was recorded 500 ms before the first trial and 500 ms after the last trial of each run (about 4 min). The recording was made with low-pass filtering at 200 Hz and sampling at 625 Hz.

Co-registration of MEG and MRI

High-resolution anatomical images of each subject's whole head were taken with a 1.5-T Siemens MRI system. For each subject, T1-weighted MRI images (voxel size of $1\times1\times1$ mm^3) were collected. Before the MEG experiment, three head coils were attached to the subject's scalp, close to the nasion, the left and right pre-auricular points, respectively. The three head coils defined a coil-based coordinate system. During each recording run, the subject's head position was monitored with these three head coils. If a subject moved excessively (3 mm or more) during a run, then the recording for the run was repeated (in total five runs across all 10 subjects).

The subject's head shape was scanned using a 3D digitizer (Fastrak, Polhemus, Colchester, VT, USA) and a 3D camera system (Vivid 700, Minolta Co. Ltd., Japan). The digitized head shape was fitted on the MRI to get a transformation matrix between coil- and MRI-based coordinate systems using Rapid Form (INUS Co. Ltd., Korea) and dedicated in-house software (Hironaga et al., 2002). The co-registration accuracy was manually checked and matched up within 1–2 mm. If the error of the fit was more than 3 mm, the digitization process was repeated.

MEG signal processing

Off-line, environmental noise was first removed from the MEG signal by forming the third gradient of the magnetic field. The resulting data were filtered using the CTF software in the 1–200 Hz band with notch filters to eliminate noise at 50 Hz and its harmonics from the power line, and at 90 Hz and its harmonics from the data projector. We then extracted trials from each run. For the task runs, we extracted data from 500 ms before the first stimulus onset to 300 ms after the test figure onset; for the figure baseline runs, we used data from 500 ms before to 1 s after the first stimulus onset. Trials with blinks and eye movements (as indicated by the EOG signals) around the image presentation (300 ms before the first stimulus onset to 200 ms after the test figure) were rejected manually. Fewer than 3 trials were rejected for eight subjects and 5 to 10 trials were excluded in some runs for two subjects in the 64 trials per run. Of the remaining extracted MEG data, subjects' artifacts such as heart function and eye blinks and movements (not around the image onset) were also removed using independent component analysis (ICA) (Jahn et al., 1999). In each of the 16 task runs and two figure baseline runs, the ICA-cleaned data were averaged on the second stimulus onset (i.e. the composite figures in the task runs and the blank screen in the figure baseline runs), based on the preceding first stimuli. In the task runs there were five averages for each composite figure A and B (AG, AL, AM, BG, BL, BM, SQA, SQB, FSA and FSB). In the figure baseline runs, there were eight averages (AG, AL, AM, BG, BL, BM, SQ and FS). There were eight trials in each averaged signal. If there were fewer than five trials available for averaging for a condition, this condition was not included in further analyses. Since the purpose of this study was to examine the priming effect of the first stimuli on the interpretation of the second partially occluded figures, we report here data from 100 ms before to 300 ms after the composite figure onset (as highlighted by the gray box in Fig. 1C).

MFT analysis

MFT is a distributed source method, producing probabilistic estimates for the non-silent primary current density vector $\mathbf{J}(\mathbf{r},t)$ at each time slice of the MEG signal (Ioannides et al., 1990). The MFT algorithm relies on a *nonlinear* solution to the inverse problem, which has optimal stability and sensitivity for localized distributed sources (Taylor et al., 1999). The MFT method has been validated by computer-generated data (Ioannides et al., 1990), implanted dipoles in humans (Ioannides et al., 1993), and numerous applications to real auditory, somatosensory and visual data sets (Ioannides et al., 1995; Ioannides, 2001; Moradi et al., 2003). For each subject, four hemispherical source spaces were defined, each covering the left, right, superior and posterior part of the brain well. Sensitivity profiles (lead fields) used for the MFT analysis were computed from a spherical head model for the conductivity of the head, defined separately for each one of the four source spaces. The center of the sphere was chosen by a best fit to the local curvature of the inner surface of the skull below a set of 90 MEG channels. MFT was used to extract activity separately from the signal corresponding to the 90 channels selected for each of the four source spaces. The spatially overlapping estimates from the four source spaces were then combined and stored in an $8\times8\times8$ mm grid covering the entire brain. For each subject, we applied MFT to the eight averages in each of the 16 task runs, from 100 ms before to 300 ms after the composite figure onset at a step of 1.6 ms. The MFT solutions produced probabilistic estimates for the instantaneous current density $\mathbf{J}(\mathbf{r},t)$ throughout the entire brain, capturing time-locked activations evoked by the composite figures. For comparison, the same MFT analysis was also applied to the blank screen onset in the two figure baseline runs, in which the blank screen replaced the composite figures in the task runs.

Post-MFT statistical parametric mapping analysis

There are two ways that the processing of a stimulus can be influenced by context: in our case the priming effect of first stimuli. The priming effect could correspond, firstly, to activation that changes its location and/or timing depending on the prime. We tested this by comparing directly the responses to composite figures with different priming stimuli (e.g. AG vs. AM) and found no significant spatiotemporal differences that were consistent across subjects. The second possibility, the one usually associated with priming, is a modulation of the overall response in one or more task specific areas. To test for this possibility, we compared MEG responses to primed and non-primed (composite) stimuli. To constrain the search for priming related effects, we first identified brain regions showing a visually evoked response to the composite figure by comparing all responses to the composite figure against a null stimulus (the blank screen in figure baseline trials). To ensure that there was no anatomical bias in our interrogation of the data, we used statistical parametric mapping in conjunction with MFT to characterize responses at all points in peristimulus time throughout the brain. Having identified regionally specific visual evoked responses we looked at the significance of the priming related effects in these areas.

In short, we analyzed the MEG data as follows. First, we used subject by subject statistical analysis of the tomographic solutions to identify task specific areas. Second, we used transformation to the Talairach space to identify common task specific areas across subjects. Third, we defined for each subject the corresponding task specific area and computed the time course of activity.

Fourth, we compared the activations corresponding to primed and control trials in task runs and thus identified brain areas sensitive to the priming manipulation.

The MFT analysis of the average signal produced estimates for the current density vector at each source space grid point and time slice for each condition in each run of each subject. All average signals were from more than five trials and most were based on eight trials. The basic elements for the statistical analysis were the modulus of the current density vector at each grid point and each time slice for each condition. We tested whether two distributions of such elements were same or different. In general the two distributions from two conditions (e.g. the second stimulus, a composite figure in task runs versus a blank figure in figure baseline runs) had different sizes. We used the unpaired *t*-test for each comparison because this test takes into account the size of each distribution. This test is the quotient of two terms. The nominator is the difference of the mean values while the denominator is the standard error obtained from the pooled variance of the two samples. The comparison was done for each grid point and at each time slice (from −100–300 ms relative to the composite/blank figure onset). We applied the conservative Bonferroni correction to obtain a *P*-value corrected for multiple comparisons across grid points. The *P*-value corresponded to the confidence level for rejecting the null hypothesis of no significant change of activity in the MFT moduli between the task and figure baseline runs. The sign of the change was then inspected: a positive *P*-value was retained if the change was positive (i.e. task higher than figure baseline), or a negative *P*-value was used to mark decrease of activity. We did not apply correction for multiple comparisons across time slices because the statistical analysis was already conservative and the results showed statistical significance in sequential latency ranges. The statistical significance achieved for each subject was extremely high and would easily survive double Bonferroni correction (for spatial and temporal repetitions of the *t*-test). We used the Bonferroni correction only for the spatial dimension when combining across subjects (see next sub-section) because we were interested in identifying the first time slice in each of such sequences with high temporal accuracy. We stress that this statistical analysis makes no a priori assumptions about any regional activity or timing because it identifies loci of significant changes of activity in a model-independent manner: grid point-by-point statistical analysis throughout the entire brain for each time slice. We describe next each statistical test used in this paper and provide details about the size of each distribution.

First, we identified brain areas and latencies where the activations were significantly different for composite figures in the 16 task runs as compared with the blank screen in the two figure baseline runs, with both preceded by identical first stimuli. The analysis was done for each subject separately. Across the 16 task runs, there were 10 conditions, corresponding to the 10 possible stimuli presented before the composite figure (six simple figure conditions: AG, AL, AM, BG, BL and BM; four control figure conditions: SQA, SQB, FSA and FSB). In each of the 16 runs, all simple figure conditions were presented and so each condition had 16 repetitions in total. But for the control figure condition, it was presented either before composite figure A or B in one run, e.g. SQ before A, FS before B, so in this run, only SQA and FSB conditions were present. Thus each of the control figure condition had eight repetitions in total. Across the two figure baseline runs, there were eight conditions, corresponding to the eight possible stimuli presented before the blank figure (AG, AL, AM, BG, BL, BM, SQ and FS). A separate test was made for each condition from the task as compared with the same condition from the baseline run. The first distribution was made of 16 (e.g. for AG condition) or eight elements (e.g. for SQA condition), one element for each repetition from the 16 task runs. The second distribution was made of 500 elements, 250 from each baseline run. The 250 elements were from the whole 400-ms period, with a 1.6 ms separation between elements.

Second, we examined the priming effect of the first stimulus on the second. That is, for the same composite figure, is there a difference in the interpretation of the occluded figures when they are preceded by simple figures (G, L or M) versus control figures (SQ, FS)? For each subject across the 16 task runs, 12 comparisons were made from the four control figure conditions and the six simple figure conditions: FSA vs. AG/AL/AM, then SQA vs. the same list. Next FSB vs. BG/BL/BM, then SQB vs. the same list. The *t*-test was computed between two distributions: the first distribution consisted of eight elements from the eight repetitions for each control figure condition, while the second distribution contained 16 elements from the 16 repetitions for each simple figure condition.

Common significantly activated areas across subjects

For each subject, we used post-MFT statistical analysis to obtain maps showing significant changes in activity at each time slice between two conditions. These individual maps were then transformed to a common Talairach space (Talairach and Tournoux, 1988). We used the following three steps to identify common significantly activated areas across all the subjects. First, for each subject, positive and negative *P*-values at each source space grid point and time slice were transformed to new values (*Q*-values) by taking the natural logarithm [$Q=\ln(P)$] and then smoothed separately by a spatial smoothing algorithm based on the sigmoid weight function:

$$Q_{\text{smoothed}}=\frac{\sum_i W_i Q_i}{\sum_i W_i}$$

where

$$W_i=\frac{1}{1+\exp\left[(R_i-c)/\alpha\right]}$$

Q_{smoothed} is the new smoothed value; Q_i is the value at the ith grid point located within a search radius of 1.5 cm from the smoothed point; R_i is the distance between the ith and the smoothed point; c and α are constants specified by the user, defining the shape of the sigmoid weight function. For the present study, we used $c=0.7$ cm and $\alpha=0.2$ cm. For each grid point, the highest Q_{smoothed} (least significance) over the time window of 6.4 ms was selected, separately for the positive and negative *P*-values. The smoothed *P*-value was then obtained as $P=\exp(Q_{\text{smoothed}})$ with the appropriate sign signifying increase or decrease of activity. Note the above spatial smoothing was only applied when we searched for common significantly activated areas across subjects, i.e. we did not alter MFT solutions and post-MFT statistical analysis results for individual subjects. Second, across all subjects, for each grid point, we calculated percentages of commonality (0–1) as follows: percent_pos$=N_{\text{pos}}/N_{\text{cases}}$, percent_neg$=N_{\text{neg}}/N_{\text{cases}}$ where N_{cases} is total number of cases ($N_{\text{cases}}=10$ subjects$\times$number of conditions from each subject), and N_{pos} and N_{neg} are the respective number of cases where significant increase or decrease in activity was identified at the predefined threshold ($P<0.05$ in this study). Third, for each grid point, we selected the higher absolute value between percent_pos and percent_neg as the output (retaining the appropriate sign).

Regions of interest (ROI) and activation time courses

The MFT solutions provided estimates for electrical sources across the entire brain millisecond by millisecond. The post-MFT

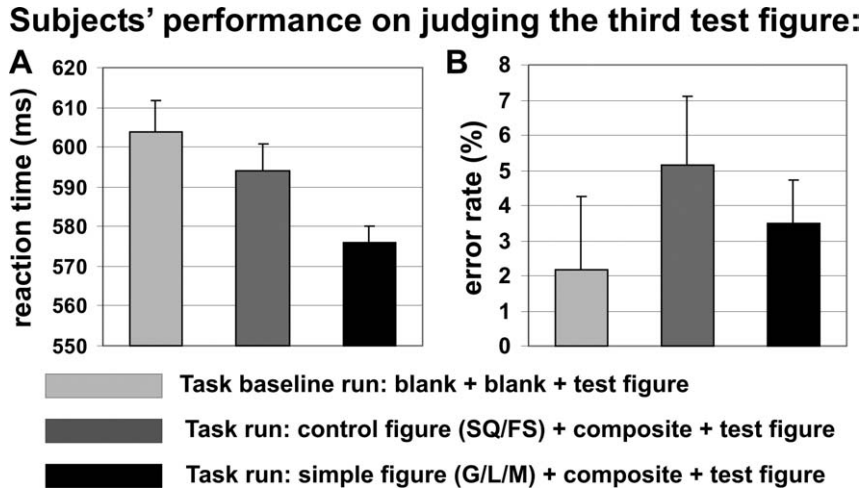

Fig. 2. Mean RT (A) and error rate (B). Behavioral data were averaged from the 10 subjects for task baseline runs, as well as for task runs in which simple (G/L/M) and control figures (SQ/FS) preceded composite and test figures. Error bars indicate 2 standard errors.

statistical analysis was then used to form unbiased basis for selecting ROIs. Specifically, we used the foci of common significantly activated areas across subjects to guide the definition of ROIs for each subject based on functional criteria. First, these common foci were labeled by their anatomical locations (e.g. the fusiform cortex) and then projected back to each subject's MRI based on the Talairach coordinates of the foci. Second, around the projected foci, for each subject, we identified by purely functional criteria the subject specific foci of maximal activity from the averaged current density vector (smoothed with a moving window of 6.4 ms in a step of 3.2 ms) over the MFT solutions for each of 10 conditions (AG, AL, AM, BG, BL, BM, SQA, SQB, FSA, FSB) in the 16 task runs. Since the functional foci defined from each condition were similar in location, we used the same ROI for all the conditions. Third, we defined ROIs as spheres centered on the functionally defined foci with radii of 1.0 cm. Finally, for each of 10 conditions in the task runs, we calculated an ROI activation time course $M(t)$ from the modulus of the current density vector as a function of time, where

$$M(t)=\int_{\mathrm{ROI}}\sqrt{\mathbf{J}(\mathbf{r},t)\cdot\mathbf{J}(\mathbf{r},t)}\,d^3\mathbf{r}.$$

RESULTS

Behavioral results

We compared subject behavioral responses to the test figures from task baseline runs with those from task runs to establish the priming effect on the third stimulus when the first two stimuli were related to it. In both task baseline and task runs subjects made judgment on the test figure by raising the left or right index finger. In task baseline runs, two blank screens preceded the test figure. In task runs, two stimuli were shown before the test figure. In one case, the first stimulus was a simple figure, which primed the interpretation of the composite second and the judgment of same–different in the third; in the other case, the first stimulus was a control figure, unrelated to the following composite figure and test figure. Behavioral responses from "same" trials provided evidence of a priming effect on the second stimulus by the first (Plomp and van Leeuwen, in press). In the present MEG study, subjects' RT showed a clear priming effect as well (Fig. 2A): RTs were significantly *reduced* by the congruence of the first two figures with the third test figure (task baseline, control and simple figures in task runs), $F(2, 18)=5.24$, $P<0.016$ in a one factor repeated measures ANOVA. In a subsequent ANOVA we also included two more factors of the test figures to assess the presence of interactions. These two factors were (1) test figure type (G, L and M) and (2) test figure shape (A and B). The three factor ANOVA confirmed the significant effect of congruence, $F(2, 18)=5.4$, $P<0.01$. No interaction between the congruence and the other two factors was observed. There was an additional main effect of test figure type, $F(2, 18)=44.4$, $P<0.001$, due to longer response times for mosaic test figures. Test figure type interacted with shape, $F(2, 108)=16.0$, $P<0.001$. Local and mosaic test figures yielded similar RTs for shapes A and B but global test figures of shape B had longer RTs. No other effects reached significance levels.

None of the subjects showed a speed-accuracy tradeoff. Error-rates were nevertheless analyzed in the same way as RT. The error rate depended on congruence, $F(2, 18)=11.4$, $P<0.001$ in a one factor repeated measures ANOVA. As depicted in Fig. 2B: the error rate was similar between simple figures (mean error rate 3.5%) and control figures (mean 5.2%) in the task runs. In comparison, task baseline trials (mean 2.2%) had a lower error rate than simple figures did. This may be because in the task baseline runs the blank stimuli were presented before the test figures so the subject experienced less cognitive loading, while in the task runs the first two stimuli preceded the test figure and so degraded performance. The three factor ANOVA confirmed the significant effect of congruence, $F(2, 18)=9.16$, $P<0.01$, and a second main effect of test figure type, $F(2, 18)=9.16$, $P<0.01$, indicating increased error rates for mosaic test figures.

The effects of RT and error-rate on test figure type were in agreement; responses to mosaic test figures were more difficult and took longer. The task baseline runs had

longest RTs due to lack of priming but lowest error rates due to reduced cognitive load. Most importantly, there was a congruence effect within task runs: RTs were longer when only the composite figure was congruent to the test figure than when both simple and composite figures were congruent to the test figure (control vs. simple figures in Fig. 2A). This replicates our earlier findings from a recent behavioral study (Plomp and van Leeuwen, in press) and suggests that processing of the composite figure is biased by the preceding first stimulus. The current RT results justify an analysis of the evoked responses of the composite figures under different priming conditions, e.g. control versus simple figures in the task runs. Furthermore, we examined the role of learning on subjects' performance. As the experiment progressed, average RTs across subjects were constant but the error rate dropped, which indicated that some learning may have occurred during the experiment. In a recent study of MEG responses to primed and non-primed composite figures (i.e. simple vs. control figures) (Plomp et al., in press), we specifically checked if learning influenced the evoked response. We found no evidence of such an effect; learning only affected the accuracy of behavioral responses to the third test figures, not the evoked response to the second composite figures. The following analysis was therefore performed across runs on the MEG response.

MEG signal

We compared the averaged MEG signal around the onset of the composite figures. These were preceded by the respective six simple figures and two control figures (AG, AL, AM, BG, BL, BM, SQA or SQB, FSA or FSB) in each task run. For each subject, 128 averages (eight conditions×16 runs) were constructed from eight trials in each condition within a run. Fig. 3A–B shows the typical signal waveform from condition AG, run 1, subject 1. Within 250 ms after the composite figure onset, the MEG signal showed peaks or dipolar patterns from 80 to 210 ms (Fig. 3A), observed mostly at occipital and temporal areas (Fig. 3B). We further analyzed the latencies and amplitudes from the 10 most representative sensors which were selected in an objective, data-driven manner. Specifically, first for every condition in each task run of every subject, we computed for each MEG sensor signal-to-noise ratio (SNR) in a 20 ms window with the center of the window moving every 1.6 ms from 50 to 300 ms after the composite figure onset. Then for every condition across all 10 subjects, we identified 10 sensors that showed the highest SNR. This resulted in a selection of 16 sensors that most consistently responded the strongest to the composite figure across all subjects. The mean SNR across the 16 sensors was 6.0 (S.D.=3.4). For each of the 16 sensors, we analyzed the latencies (Fig. 3C) and amplitudes (Fig. 3D) of the largest peak in the 50–300 ms interval. For

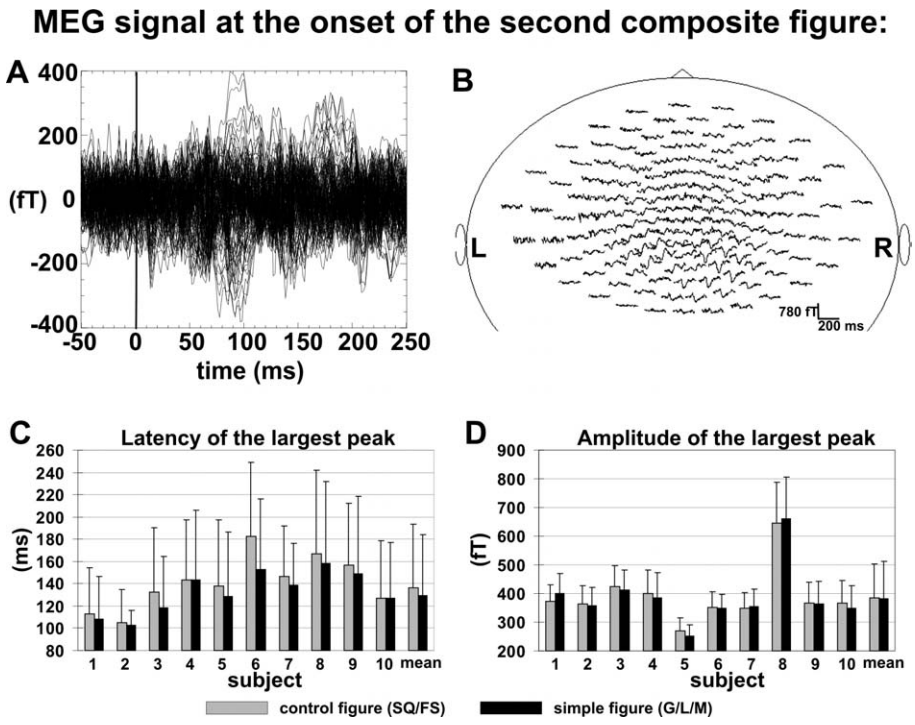

Fig. 3. Typical MEG signal waveform (A, B) and analysis of latency and amplitude of the signal (C, D). (A, B) The signal was averaged from subject 1's first run on the onset of composite figure A preceded by its simple figure AG (eight trials). Data were plotted from −50–250 ms relative to the composite figure onset, with all 151 MEG channels shown superimposed in (A) and channel-by-channel in a head model in (B). From the MEG signals, the latency (C) and amplitude (D) of the largest peak between 50 and 300 ms after the onset of the composite figure were compared between primed (simple figures) and unprimed (control figures) condition. In (C, D), results for individual subjects were first plotted and then the overall mean across all 10 subjects. Error bars indicate 1 standard error.

composite figures preceded by simple figures, as compared with control figures, we found that the latencies were significantly *shorter* (mean 129.5 versus 136.4 ms), $F(1, 9)=33.0$, $P<0.001$, in a repeated measures ANOVA with two factors, (1) congruence of the first stimulus with the second composite figure (control and simple figures) and (2) composite figure shape (A and B). The amplitudes were marginally *lower* (mean 382.7 versus 384.5 fT, $F(1, 9)=3.4$, $P<0.1$). No interaction effects were observed.

We have reported elsewhere a direct comparison of the MEG signals for composite figures preceded by the three types of simple figures: global, local and mosaic primes (Plomp et al., in press). We found reduced latency and increased amplitude for the evoked response of the second composite figure when the preceding stimulus was a mosaic as compared with either local or global interpretation of the occluded figure. The earliest mean latency for mosaic first figure was 119 ms while for global and local first figure it was 125 ms.

Activated brain areas and timing of activation

Using MFT analysis of the MEG signal, we were able to follow activity across the entire brain millisecond by millisecond. Following the composite figure onset, activations were observed in widespread occipital and temporal areas. Post-MFT statistical analysis showed significant changes in activity between conditions for each of the 10 subjects. These individual significance maps were then transferred to a common Talairach space and percentages of commonality were calculated to evaluate across all the subjects and conditions how common the significant activations were.

We first identified brain areas and time periods where the activity was significantly different between the composite figures in the task runs and a blank screen in the figure baseline runs, with both the composite and blank figures preceded by the same first figures. Fig. 4 shows the most common significant difference in the whole brain by combining results from the 10 comparisons (AG, AL, AM, BG, BL, BM, SQA, SQB, FSA and FSB) in each subject. The common areas were around bilateral V1/V2 and lateral occipital complex (LOC), and right fusiform gyrus (FG). For completeness, we also showed the left fusiform area. The numbers at the bottom of each panel denote the percentage of commonality from the 100 cases (10 comparisons×10 subjects). Based on these common significantly activated areas, we defined three pairs of areas, one in each hemisphere, as ROI. ROIs were defined functionally and separately for each subject based on the MFT solution, as shown for subject one with white circles in Fig. 4. The Talairach coordinates for the ROIs (x, y, z in mm; mean±S.D.) from all 10 subjects are listed in the table at the lower part of Fig. 4.

Priming of occluded figure interpretation

Fig. 5 shows the activation time courses for V1/V2, LOC and FG bilaterally, 100 ms before to 300 ms after the composite figure onset. For each ROI, we calculated the grand-averages across all 10 subjects for each of the

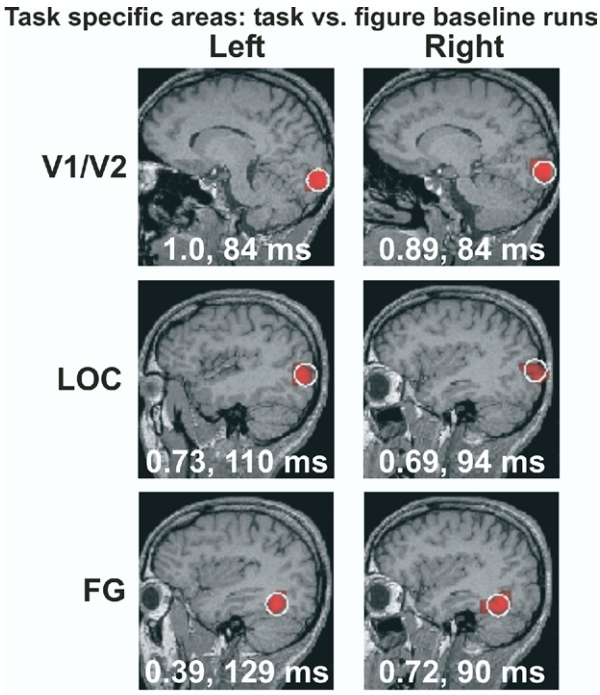

Talaraich coordinates (x, y, z) ± s.d. in mm:

ROI	Left hemisphere	Right hemisphere
V1/V2	-10 ± 2, -83 ± 2, -6 ± 9	11 ± 3, -83 ± 5, -1 ± 6
LOC	-39 ± 3, -72 ± 4, 7 ± 6	37 ± 2, -71 ± 2, 7 ± 7
FG	-33 ± 2, -51 ± 4, -13 ± 3	34 ± 3, -50 ± 5, -12 ± 3

Fig. 4. Statistical maps for the comparison of composite figures in the task runs with the blank screen in the figure baseline runs. Result from 10 subjects, superimposed on the structural MRI from subject 1. Common areas of differential activation are around calcarine sulcus (V1/V2), LOC and FG. Numbers at the bottom of each panel denote latencies and the percentages of commonality, with 1.0 signifying all 10 conditions in each of the 10 subjects having significant change in activity for the comparison ($P<0.05$) around the identified area and latency. White circles represent ROIs that we defined from the common significant change in activity. Talairach coordinates for the ROIs are listed in the table at the lower part of the figure.

simple and control figure types preceding the composite figure, as shown in different colors in the figure. Notably, across all the ROIs, only the activation in the right FG (bottom right in the figure) showed a marked difference between the simple and control figures in the task runs: the activation for the primed trials (G/L/M) was *reduced* in comparison with the control trials (SQ/FS) between 120 and 200 ms. We applied ANOVA to determine whether the marked difference between the two groups of trials is significant or not. The analysis was based on the right FG ROI activation integrated in the latency range of 100–200 ms, with two factors (1) composite figure shape (A and B) and (2) group (simple and control trials). We found significant main effect of group ($F(1,1262)=74$, $P<0.00001$) and an interaction between group and shape ($F(1,1262)=5.3$, $P<0.05$). An additional multiple comparison test (Scheffé post hoc test) showed that the differences between simple and control trials for shape A or B were significant ($P<0.0005$), but the differences between

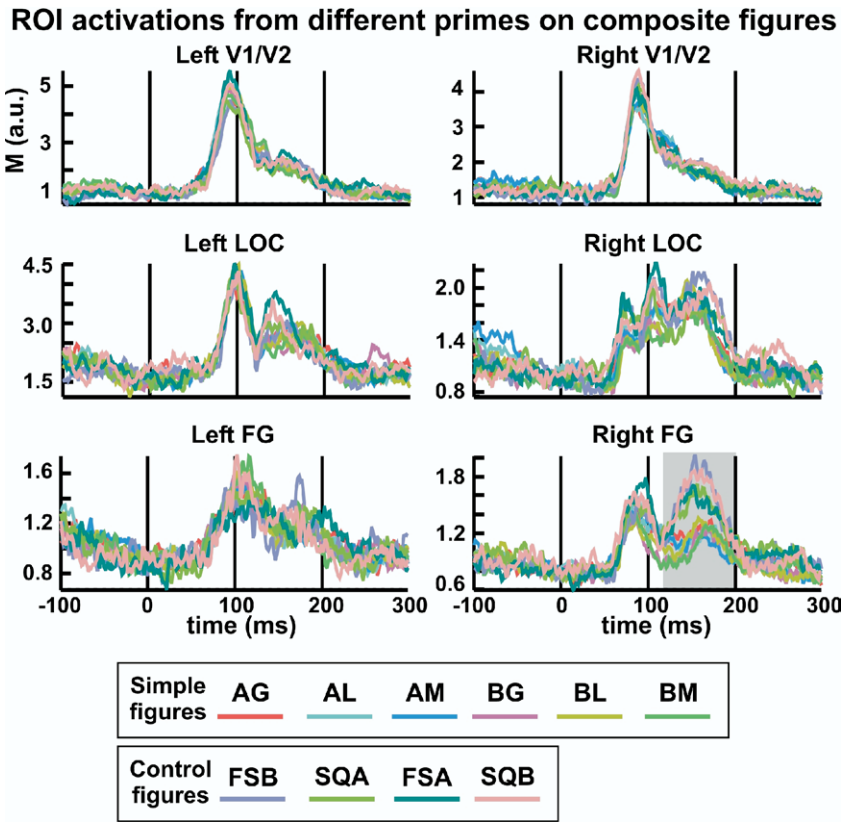

Fig. 5. Activation time courses for ROIs around V1/V2, LOC and FG in both hemispheres. Curves were averaged on composite figure onset for each of the 10 first stimulus types (shown in different colors) for all 10 subjects. Simple figures led to significantly reduced activity in the right FG compared with control figures between 120 and 200 ms, as highlighted by the gray box. Note vertical scale is different for each panel.

shape A and B for simple or control trials were not ($P<0.6$).

The significant difference between the two groups of trials preceding the composite figures was also identified in our post-MFT statistical analysis. Fig. 6 shows the common significant differences in activity during task runs for comparisons between control (SQ, FS) and simple figures (G, L, M) preceding the same composite figure A or B (e.g. FSA vs. AG, FSB vs. BL, SQA vs. AM and so on). For composite figures preceded by simple figures, as compared with control figures, all 12 comparisons showed significantly *reduced* activity for at least 5 of the 10 subjects around the right posterior fusiform area. No other brain areas showed such a systematic change in activity. The reduced activation was observed in two time ranges: 81–116 ms and 132–174 ms, with higher percentages of commonality (more subjects) in the latter time range. Note that the number of subjects showing the above significant difference in the right fusiform area was obtained from the statistical analysis performed on the MFT instantaneous solution every 1.6 ms and source space grid point over the entire brain. Note also the latency ranges in Figs. 5–6 are from specific ROIs while in Fig. 3C they are from the MEG signal of the most responsive sensors, observed mostly at the occipital area.

DISCUSSION

The primed same–different task

We used a same–different task in which subjects were shown rapid sequences of three stimuli: a simple or control figure, a composite with a partially occluded shape, and a test figure. The first simple figure was the global or local completion, or the mosaic interpretation of the occluded figure. The third stimulus was the decision target of the task: a pair of simple figures that could be identical or different. Using a sequence of three stimuli allowed us to obtain a perceptual priming effect on the second stimulus, independent of decision-related processing, which was done on the third stimulus. The behavioral data analysis evaluated the priming effect of the preceding stimuli on RT to “same” trials. When the first prime figure and the second composite figure were congruent to the test figure, subjects responded significantly faster than when control figures (as in the task run) or blank figures (as in the task baseline runs) preceded the test figure (Fig. 2A). The behavioral results, therefore, showed a clear priming effect. Although they were obtained on the third test figure, instead of directly on the second stimulus, evidence from our previous behavioral study showed that the second stimulus is primed as well. When evaluating the condition in which simple and composite figures were both congru-

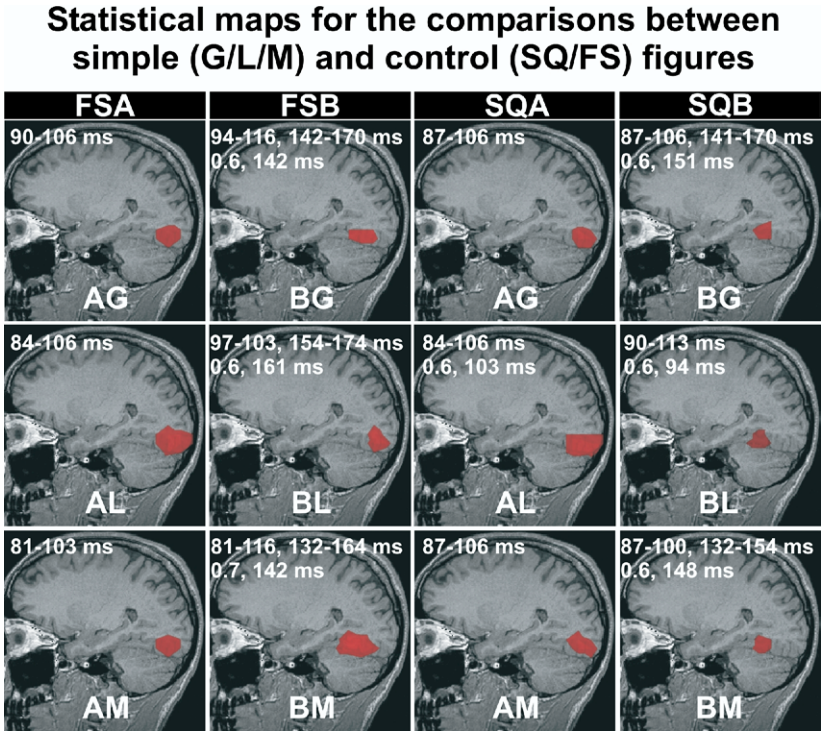

Fig. 6. Priming of occluded figure interpretation by comparing simple with control figures. Both types preceded the same occluded composite figures in task runs. The most common significant changes in activity when comparing simple (G/L/M) with control (SQ/FS) figures. Right FG was the only common area. Top numbers in each panel denote time ranges in which significant activations are common to at least half of all the comparisons (0.5) and, if greater than 0.5, the bottom numbers indicate the highest percentage of commonality in each comparison and its corresponding latency.

ent with the test figure against cases where only one or none were congruent, a super-additive priming effect from the preceding two figures on the third was obtained. In that case the reduction in RT was larger than the summed individual priming effects (Plomp and van Leeuwen, in press).

The corresponding evoked MEG signal of the second composite figure in the present study showed this priming effect on the second stimulus directly: for the largest peak between 50 and 300 ms after the composite figure onset, the latencies were shorter and the amplitudes were lower for composite figures preceded by simple as compared with control figures (Fig. 3C–D). The most parsimonious explanation for the changes of the MEG signal is that in primed trials, brain activity in areas playing a key role in the occluded figure interpretation was earlier and reduced.

The priming effect on the occluded figure interpretation reported in this work cannot be explained by overlap in features between prime and composite figure because one of the control figures was SQ which had more overlap with the composite than the simple figures. The fact that the priming effect was not observed in the control condition (Fig. 5) further confirmed that our experimental design was appropriate to address the question of priming on occluded figure interpretation.

Interpretations of occluded figures

A composite figure can be interpreted as a mosaic or a partially occluded figure. The occluded figure can be completed locally or globally behind its occluder. Some psychophysical studies suggest that occluded objects may initially be represented as mosaics (Sekuler and Palmer, 1992; Murray et al., 2001), others report no evidence for an initial mosaic representation prior to completion, that is, the representations begin to evolve toward completion almost immediately (Bruno et al., 1997). Furthermore, according to Sekuler and Palmer (1992), the visual system requires 100–200 ms of processing time before the representations of objects with 25% contour occlusion correspond to completed forms. On the other hand, Murray et al. (2001) suggested that the completion of partially occluded objects could occur within 75 ms. The existence of these variations suggests that the time required for visual object completion may not be fixed within the visual system; instead it changes with a number of factors such as task requirement, individual differences among subjects and stimulus variables.

On the other hand, the great variability of completion duration estimates obtained in these studies suggests that aggregate measures such as RT may not have sufficient resolution to determine the time course of perceptual completion. In addition, they failed to make an appropriate distinction between perceptual completion and decision stages. In the present study we have made efforts to remedy both problems. First, decision was separated from perceptual priming by using a sequence of three stimuli. Second, brain activity was studied with fine spatiotemporal resolution. Our result shows that a specific area, the right

fusiform cortex, acts as a hub for different interpretations (local and global occlusions as well as mosaics) in an early perceptual stage, between 120 and 200 ms after the onset of the composite figure.

We note that for our presentation times (50 ms) a completion was unlikely to be formed while the figure was on screen. The reason why we chose this short presentation time was because our recent behavioral study showed that the priming effect, the first simple figure biased the processing of the second composite figure toward one of its interpretation, was only observed when the composite figure was presented briefly for 50 ms (Plomp and van Leeuwen, in press).

Had there been a clearly distinct mosaic stage, we should have observed an earlier effect of primed mosaic than of primed completion interpretations. This however was not evident; the MEG data as analyzed here showed that all the three different figure interpretations can be equally primed in the fusiform cortex between 120 and 200 ms after the composite figure onset (Figs. 5–6). No other areas within the visual system showed a differential response to mosaic primes at the same latency across subjects. Yet, our MEG data provide some evidence of a special status for the mosaic prime in the early part of the completion process. In the latencies just preceding the clear priming effect in the right FG, we found that mosaic prime reduced the latency and increased the amplitude of evoked MEG signal more than the local and global primes (Plomp et al., in press). In the present study, direct comparisons between the tomographic estimates of activity for the different primes (global, local and mosaic) showed significant differences in striate and extrastriate areas, but at different latencies and in different areas (even hemispheres) for individual subjects. These preliminary results suggest that processes relating to a mosaic interpretation of the occlusion figure can dominate in an early stage of visual processing. These processes should involve interactions between areas and they do not lead to single focus of preferential activation at a common latency range. We are using mutual information analysis to identify how the different primes influence the analysis of the composite figure and the results will be described in a future publication. At any rate, the dependence of activity on the type of the priming stimulus ends by about 130 ms, at least at the level of analysis used in the current study and in accordance with Plomp et al. (in press).

Activation areas related to occluded figure processing

Understanding the role of priming on occluded figure interpretation requires high-resolution spatial and temporal information about brain activity. MEG offers the required resolution. Spatially, it approaches that of fMRI, at least for superficial generators, while its temporal resolution is far better, allowing the evolution of brain activity to be tracked millisecond by millisecond. In two recent MEG studies, we demonstrated accurate localization at both cortical (Moradi et al., 2003) and sub-cortical levels (Ioannides et al., 2005). In the present study, we used the same tomographic analysis (MFT) as in these earlier studies. Applying post-MFT statistical parametric mapping, we further identified brain areas and latency periods when the activity was significantly different between the task and figure baseline runs or between two conditions in the task runs. The loci of significant change in activations were defined in a model-independent manner. Following the onset of the composite figures, occipital and temporal areas were activated (Fig. 3–4). The comparison between the task and figure baseline runs showed that the composite figures elicited significant change in activity compared with a blank screen around the calcarine sulcus, LOC and fusiform gyri (Fig. 4). The identified LOC and FG areas were in excellent agreement with those reported in other earlier fMRI studies on amodal completion (Lerner et al., 2002) and priming (Buckner et al., 1998; James et al., 2000; Henson et al., 2000; Koutstaal et al., 2001; Vuilleumier et al., 2002; Simons et al., 2003; Reber et al., 2005).

Timing of occluded figure processing and priming effects

Two recent event-related potential (ERP) studies of amodal completion provide some information on timing. Using illusory shapes, Murray et al. (2004) found activations within lateral occipital and posterior parietal cortices from 140 to 300 ms. Using successively less fragmented images, Doniger et al. (2000) found that bilaterally in occipitotemporal areas the perceptual closure processes leading up to object recognition started at 230 ms and peaked at 290 ms. The onset latency difference from the two ERP studies may be due to the fact that more complex stimuli and a different task were used in the Doniger et al. (2000) study. In the present work, we observed stages of activations during occluded figure processing in the occipitotemporal areas (Fig. 5). Peak activity started in V1/V2 at 90 ms, in LOC at 100 ms on the left and 110 ms on the right, and in FG at 110 ms on the left and 160 ms on the right. Interestingly, in the right hemisphere, slightly weaker activations in LOC and FG were also present at about 80 ms and 90 ms, respectively. These latencies fit well with the estimated required time to completion of occluded objects (60–200 ms) from previous psychophysical studies (Sekuler and Palmer, 1992; Murray et al., 2001). An ERP study of illusory contour (IC) processing (Murray et al., 2002) reported that IC stimuli resulted in modulation of early visual evoked potentials (88–100 ms) over lateral occipital scalp bilaterally.

Recent monkey studies showed that neural response suppression is rapid, with an onset latency in perirhinal neurons that equals their visual response latency (70–80 ms), and the mean population latency may be as short as 150 ms (Ringo, 1996). These latencies are considerably shorter than the latencies of priming-related effects measured with ERPs in humans, typically with onset around 250–300 ms (Rugg and Doyle, 1994). Although human intracranial ERP recordings in inferior temporal regions show early object-specific (e.g. face-specific) potentials at 150–200 ms after stimulus onset (Allison et al., 1999), little evidence has shown that these potentials are sensitive to

prior experience with objects. With our present MEG work, we showed that the onset latency of priming started from 120 ms, peaked at 160 ms and dissipated before 200 ms (Fig. 5). Our experimental design separated the priming effect in early perceptual stages from later decision-related stages of processing. This may explain why the onset latency of priming from our current study is shorter than earlier ERP studies of priming effects, in which the primed items were also the decision target of the task.

Hemispheric asymmetries in priming of occluded figures

Recent findings indicate a dominant role of right hemisphere in amodal completion and priming. Using callosotomy (split-brain) patients, Corballis et al. (1999) showed that amodal completion is more dominant in the right hemisphere than the left. In an ERP study, Murray et al. (2004) found a large right versus left hemi-scalp difference for amodal completion in healthy subjects.

Priming-related task facilitation has also been shown to be anatomically selective (Buckner et al., 1998; James et al., 2000). In neuroimaging studies, priming is often associated with a decrease in activation in brain regions involved in object recognition. This might be because priming causes a sharpening of object representations which leads to more efficient processing and, consequently, a reduction in neural activity. Recent fMRI studies on object priming in humans have reported reduced activation in the inferotemporal and occipitotemporal cortex after object recognition, which included the lateral occipital cortex and FG (Buckner et al., 1998; James et al., 2000; Koutstaal et al., 2001; Vuilleumier et al., 2002; Simons et al., 2003; Reber et al., 2005). More specifically, two subsystems of priming have been examined extensively, one representing form-specific information and the other representing abstract form information (Marsolek et al., 1992). Form-specific representations preserve specific characteristics of the lines of the stimuli themselves, while abstract representations specify the identity of the stimulus. More recently, psychophysical and neuroimaging studies indicate that abstract and specific visual form systems operate independently in the brain. In the left hemisphere, an abstract-category subsystem operates more effectively than a specific-exemplar subsystem, and in the right hemisphere, a specific-exemplar subsystem operates more effectively than an abstract-category subsystem (Marsolek et al., 1992, 1996; Beeri et al., 2004). Decreased activity in the right fusiform cortex associated with priming depends on whether the three-dimensional objects were repeated from the same viewpoint (Vuilleumier et al., 2002), exemplar-specificity (Koutstaal et al., 2001; Simons et al., 2003), or stimulus-familiarity (Henson et al., 2000). Furthermore, in an fMRI study, the right FG exhibited reductions in evoked response that grew in magnitude for stimulus repetitions from the second to the eighth presentations (Reber et al., 2005); this suggests a link between priming and the development of visual expertise. Our current results support a dominant role for the right hemisphere in amodal completion and priming. Using a form-specific priming task that presented a simple or control figure before an occluded composite figure, we found that priming in the interpretation of occluded figures is correlated with significantly reduced activation in the right fusiform cortex between 120 and 200 ms after stimulus onset.

Acknowledgments—We thank K. Tanaka, P. B. C. Fenwick and B. L. La Madeleine for helpful comments on the manuscript, and M. Maruyama for help with the SPSS statistical package.

REFERENCES

Allison T, Puce A, Spencer DD, Mccarthy G (1999) Electrophysiological studies of human face perception. I: Potentials generated in occipitotemporal cortex by face and non-face stimuli. Cereb Cortex 9:415–430.

Bartlett NR (1965) Thresholds as dependent on some energy relation. In: Vision and visual perception (Graham CH, ed), pp 154–184. New York: Wiley.

Beeri MS, Vakil E, Adonsky A, Levenkron S (2004) The role of the cerebral hemispheres in specific versus abstract priming. Laterality 9:313–323.

Bruno N, Bertamini M, Domini F (1997) Amodal completion of partly occluded surfaces: is there a mosaic stage? J Exp Psychol Hum Percept Perform 23:1412–1426.

Buckner RL, Goodman J, Burock M, Rotte M, Koutstaal W, Schacter D, Rosen B, Dale AM (1998) Functional-anatomic correlates of object priming in humans revealed by rapid presentation event-related fMRI. Neuron 20:285–296.

Buffart H, Leeuwenberg E (1981) Coding theory of visual pattern completion. J Exp Psychol Hum Percept Perform 7:241–274.

Corballis PM, Fendrich R, Shapley RM, Gazzaniga MS (1999) Illusory contour perception and amodal boundary completion: evidence of a dissociation following callosotomy. J Cogn Neurosci 11:459–466.

Doniger GM, Foxe JJ, Murray MM, Higgins BA, Snodgrass JG, Schroeder CE, Javitt DC (2000) Activation timecourse of ventral visual stream object-recognition areas: high density electrical mapping of perceptual closure processes. J Cogn Neurosci 12:615–621.

Henson R, Shallice T, Dolan R (2000) Neuroimaging evidence for dissociable forms of repetition priming. Science 287:1269–1272.

Henson RN (2003) Neuroimaging studies of priming. Prog Neurobiol 70:53–81.

Hironaga N, Schellens M, Ioannides AA (2002) Accurate co-registration for MEG reconstructions. In: Proceedings of the 13th international conference on biomagnetism (Nowak H, Hueisen J, GieBler F, Huonker R, eds), pp 931–933. Berlin: VDE Verlag.

Ioannides AA (2001) Real time human brain function: observations and inferences from single trial analysis of magnetoencephalographic signals. Clin Electroencephalogr 32:98–111.

Ioannides AA, Bolton JPR, Clarke CJS (1990) Continuous probabilistic solutions to the biomagnetic inverse problem. Inverse Problems 6:523–542.

Ioannides AA, Fenwick PB, Liu L (2005) Widely distributed magnetoencephalography spikes related to the planning and execution of human saccades. J Neurosci 25:7950–7967.

Ioannides AA, Liu MJ, Liu LC, Bamidis PD, Hellstrand E, Stephan KM (1995) Magnetic field tomography of cortical and deep processes: examples of "real-time mapping" of averaged and single trial MEG signals. Int J Psychophysiol 20:161–175.

Ioannides AA, Muratore R, Balish M, Sato S (1993) In vivo validation of distributed source solutions for the biomagnetic inverse problem. Brain Topogr 5:263–273.

Jahn O, Cichocki A, Ioannides AA, Amari S (1999) Identification and elimination of artifacts from MEG signals using extended independent component analysis. In: Recent advances in biomagnetism

(Yoshimoto T, Kotani M, Kuriki S, Karibe H, Nakasato N, eds), pp 224–228. Sendai: Tohoku University Press.

James TW, Humphrey GK, Gati JS, Menon RS, Goodale MA (2000) The effects of visual object priming on brain activation before and after recognition. Curr Biol 10:1017–1024.

Joseph JS, Nakayama K (1999) Amodal representation depends on the object seen before partial occlusion. Vision Res 39:283–292.

Kanizsa G, Gerbino W (1982) Amodal completion: seeing or thinking? In: Organisation and representation in perception (Beck J, ed), pp 167–190. Hillsdale, NJ: Lawrence Erlbaum Associates.

Kellman PJ, Shipley TF (1991) A theory of visual interpolation in object perception. Cognit Psychol 23:141–221.

Koutstaal W, Wagner AD, Rotte M, Maril A, Buckner RL, Schacter DL (2001) Perceptual specificity in visual object priming: functional magnetic resonance imaging evidence for a laterality difference in fusiform cortex. Neuropsychologia 39:184–199.

Lerner Y, Hendler T, Malach R (2002) Object-completion effects in the human lateral occipital complex. Cereb Cortex 12:163–177.

Marsolek CJ, Kosslyn SM, Squire LR (1992) Form-specific visual priming in the right cerebral hemisphere. J Exp Psychol Learn Mem Cogn 18:492–508.

Marsolek CJ, Schacter DL, Nicholas CD (1996) Form-specific visual priming for new associations in the right cerebral hemisphere. Mem Cognit 24:539–556.

Moradi F, Liu LC, Cheng K, Waggoner RA, Tanaka K, Ioannides AA (2003) Consistent and precise localization of brain activity in human primary visual cortex by MEG and fMRI. Neuroimage 18:595–609.

Murray MM, Foxe DM, Javitt DC, Foxe JJ (2004) Setting boundaries: brain dynamics of modal and amodal illusory shape completion in humans. J Neurosci 24:6898–6903.

Murray MM, Wylie GR, Higgins BA, Javitt DC, Schroeder CE, Foxe JJ (2002) The spatiotemporal dynamics of illusory contour processing: combined high-density electrical mapping, source analysis, and functional magnetic resonance imaging. J Neurosci 22:5055–5073.

Murray RF, Sekuler AB, Bennett PJ (2001) Time course of amodal completion revealed by a shape discrimination task. Psychon Bull Rev 8:713–720.

Plomp G, Liu LC, van Leeuwen C, Ioannides AA (2006) The "mosaic stage" in amodal completion as characterized by MEG responses. J Cogn Neurosci (in press).

Plomp G, van Leeuwen C (2006) Asymmetric priming effects in visual processing of occlusion patterns. Percept Psychophys (in press).

Reber PJ, Gitelman DR, Parrish TB, Mesulam MM (2005) Priming effects in the fusiform gyrus: changes in neural activity beyond the second presentation. Cereb Cortex 15:787–795.

Ringo JL (1996) Stimulus specific adaptation in inferior temporal and medial temporal cortex of the monkey. Behav Brain Res 76:191–197.

Rugg MD, Doyle MC (1994) Event-related potentials and stimulus repetition in direct and indirect tests of memory. In: Cognitive electrophysiology (Heinze HJ, Munte T, Mangun GR, eds), pp 124–148. Boston: Birkhauser.

Sekuler AB, Palmer SE (1992) Perception of partly occluded objects: A microgenetic analysis. J Exp Psychol Gen 121:95–111.

Simons JS, Koutstaal W, Prince S, Wagner AD, Schacter DL (2003) Neural mechanisms of visual object priming: evidence for perceptual and semantic distinctions in fusiform cortex. Neuroimage 19: 613–626.

Stins JF, van Leeuwen C (1993) Context influence on the perception of figures as conditional upon perceptual organization strategies. Percept Psychophys 53:34–42.

Talairach J, Tournoux P (1988) Co-planar stereotaxic atlas of the human brain. Stuttgart: G. Thieme.

Taylor JG, Ioannides AA, Muller-Gartner HW (1999) Mathematical analysis of lead field expansions. IEEE Trans Med Imaging 18:151–163.

Tulving E, Schacter DL (1990) Priming and human memory systems. Science 247:301–306.

van Lier RJ, van der Helm PA, Leeuwenberg EL (1995) Competing global and local completions in visual occlusion. J Exp Psychol Hum Percept Perform 21:571–583.

Vuilleumier P, Henson RN, Driver J, Dolan RJ (2002) Multiple levels of visual object constancy revealed by event-related fMRI of repetition priming. Nat Neurosci 5:491–499.

Zemel RS, Behrmann M, Mozer MC, Bavelier D (2002) Experience-dependent perceptual grouping and object-based attention. J Exp Psych Hum Percept Perform 28:202–217.

(Accepted 26 April 2006)
(Available online 6 June 2006)